ME 221 – Spring 2025

Laboratory 05 – Solar Cell

Nate Abrams, Jeffrey Harrick, and Jay Parmar

April 9, 2025

1 Introduction

This experiment aimed to construct and test a dye-activated solar cell using anthocyanin from blackberries. The experiment involved creating a TiO2 paste, coating and annealing conductive glass slides, dyeing them in blackberry juice, then assembling the solar cell with a graphite coated glass slide, acting as a counter electrode. Then voltage and current under varying resistances were taken and the power output and cell efficiencies were calculated. Using this lab, the team aims to learn how material structure and material processing affect the performance of a solar cell and reinforce in-class content.

2 Background

Dye activated solar cells are a type of photovoltaic device that harnesses energy from sunlight using principles similar to those found in the photosynthesis process. In this lab, a solar cell was constructed by coating conductive glass with a noncrystalline film of titanium dioxide (TiO2), staining it with anthocyanin dye from blackberries, and assembling it with a graphite coated counter electrode and iodide electrolyte. When this setup is expose to sunlight (or simulated sunlight), the dye absorbs photons and releases electrons, which are forced into the TiO2 layer and flow through the rest of the circuit, generating an electric current. The graphite electrolyte allows the cycle to continue by supplying the dye with more electrons. This process clearly shows the role of surface chemistry, band structure, and charge transfer in real-world applications. (Smestad and Grätzel 752–755).

This experiment is rich in materials science based content. The porous TiO2 film provides a large surface area for dye absorption and efficient electron transport. The molecular structure of anthocyanin allows them to bind to the TiO2 and absorb the photons. These interactions are necessary for maximizing the energy efficiency of the solar cell and reinforce in-class discussion of how atomic level structure affects material performance. Use of the natural dye and low cost materials highlights the accessibility of solar energy. As the world shifts toward a more green energy system, this technology will become increasingly crucial to society. Simple methods like this are being explored more in depth around the world as a basis for clean energy systems. ("How to Make a Solar Cell").

3 Experimental Procedure & Materials

In this experiment, a colloidal TiO2 suspension was prepared by grinding 6 g of Degussa P25 nanoparticles with 9.0 mL of 1 M acetic acid in a mortar and pestle for approximately 30 minutes, adding the acid in an initial 2 mL portion followed by 0.5 mL increments until a smooth, lump-free paste formed. After grinding, 3–4 drops of dilute Triton X-100 surfactant were mixed in to improve spreading, and the paste equilibrated under foil for 15 minutes. Meanwhile, quartz glass slides were cleaned with ethanol and deionized water, dried with kim-wipes, and the conductive SnO2-coated side identified using a multimeter. One slide was taped along three edges to serve as a spacer, a second clean slide placed beside it (taped on two sides), and two drops of the TiO2 colloid deposited at the open edge. A clean plastic pipette side was then used to spread the suspension evenly across both conductive faces, yielding a uniform film ready for annealing. The slide with tape on only two sides is kept and annealed on a hot plate at 540 C until the coating has darkened then become white again.

Anthocyanin dye was extracted by crushing two blackberries and mixing the pulp with 2.5 mL methanol, 0.4 mL acetic acid, and 2.1 mL deionized water. Annealed TiO2 films were immersed—film side down—in the dye solution for 10 minutes, then rinsed with DI water and blotted dry. Meanwhile, counter-electrodes were prepared by coating cleaned SnO2 slides with graphite from a pencil. Each dyed film was paired with a graphite slide, offset slightly for alligator-clip access, and secured with binder clips; 1–2 drops of iodine electrolyte were introduced at the edges to fill the interstice.

Once assembled, the cell was positioned under a high-intensity lamp and connected via alligator clips to a digital multimeter and a potentiometer to vary the external resistance (Appendix 1). Voltage and current readings were taken at several resistance settings to construct I–V and power characteristics, and the data were plotted and analyzed in the following section.

4 Results

Table 1: Voltage and Current Measurements for Specimens 1–3

Trial #	Specimen 1		Specimen 2		Specimen 3	
	Current (mA)	Voltage (V)	Current (mA)	Voltage (V)	Current (mA)	Voltage (V)
1	0.0043	0.101	0.0043	0.104	0.0020	0.100
2	0.0073	0.087	0.0072	0.085	0.0080	0.080
3	0.0084	0.070	0.0086	0.068	0.0105	0.070
4	0.0093	0.054	0.0094	0.055	0.0114	0.056
5	0.0097	0.038	0.0098	0.037	0.0121	0.039
6	0.0100	0.020	0.0102	0.021	0.0120	0.019
7	0.0111	0.006	0.0108	0.007	0.0120	0.002

The data in the table above shows the raw experimental data from the three specimens. Despite the fact that Specimen 2 was cracked from the annealing process all of the values appear to be similar without too much fluctuation. Seven trials were done for each specimen to ensure a fine enough granularity for analysis.

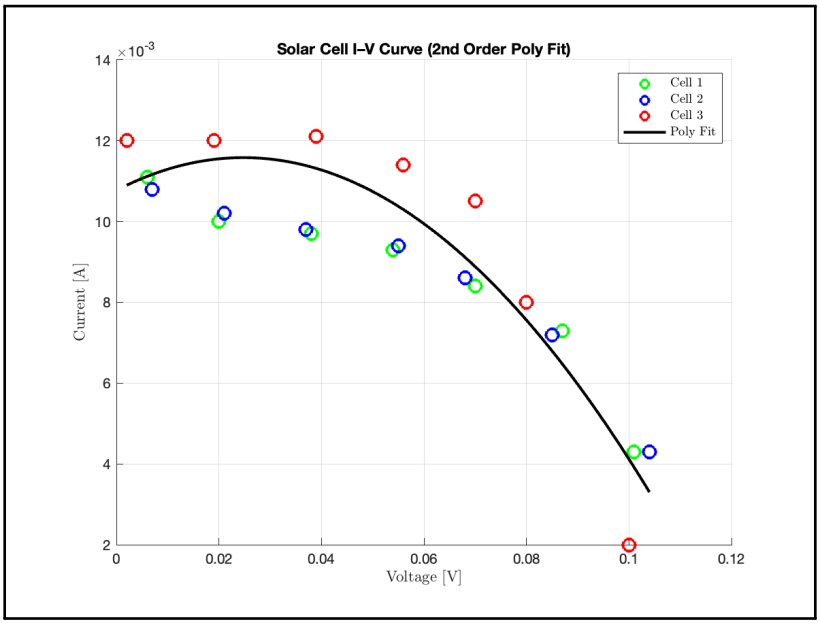

Figure 1: I-V curve with fitted line from all specimens

The I-V curve is characteristically similar in shape and conclusion to the current voltage curve from the lab manual (Appendix 2). Both curves shows a general trend that as voltage increases eventually current will approach zero as they cell loses efficiency as there is too much internal resistance. Specimen 3 outperforms the other two, yet all three follow the same trend as previously mentioned.

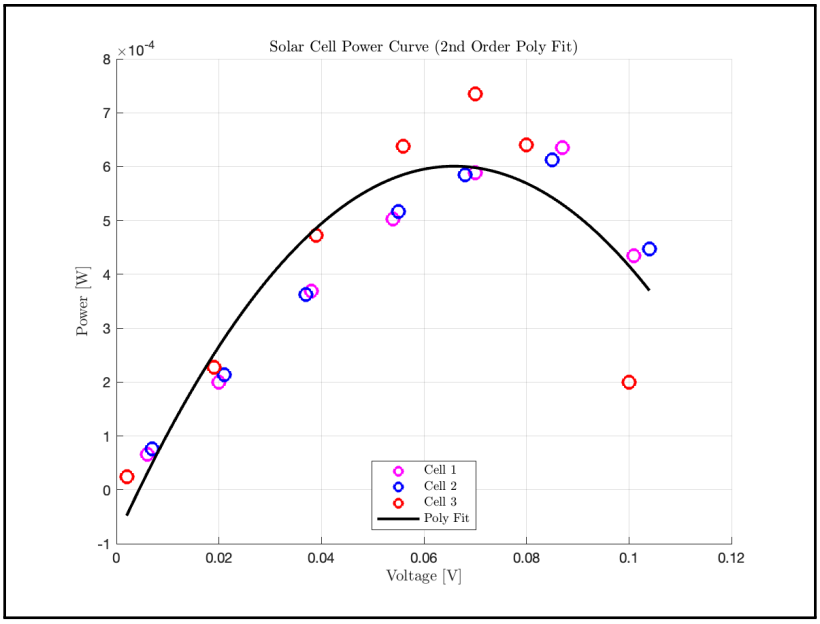

Figure 2: Power curve with fitted line from all specimens

The P–V curve mirrors the profile in Appendix 3 of the lab manual: power climbs with increasing voltage, reaches a maximum of about 6 W at 0.065 V, then falls off as internal resistance takes over. Specimen 3 again delivers the highest peak power, though all three specimens follow this same characteristic trend.

Table 2: Specimen Power output and Efficiency

Specimen	**Power Output** $\frac{W}{m^2}$	**Efficiency %**
1	3.175	0.397
2	3.060	0.383
3	3.675	0.459
Average	3.303	0.413

All specimens exhibit similar power outputs; however, Specimen 3 achieves the highest output and efficiency. The others maintain comparable values. Overall, the average efficiency aligns with reported research ($\approx 0.4\%$), and under an $800\frac{W}{m^2}$ irradiance, we measured an efficiency of 0.413%.

5 Discussion

5.1 Analysis of Results

5.1.1 Current–Voltage Relationship

The measured I–V curves for all three specimens (Figures 1) exhibit the characteristic photovoltaic behavior predicted by the lab manual: a high short-circuit current and a rapid drop in current as the cell approaches its open-circuit voltage. From Table 1, the average short-circuit current (I_{SC}) was approximately $8.97 \pm 0.7\,\text{mA}$, and the open-circuit voltage (V_{OC}) was $0.0533 \pm 0.0006\,\text{V}$. The formatted curves are in reasonable agreement with the idealized curve in Appendix 2, confirming that our TiO_2/anthocyanin architecture successfully injects electrons into the TiO_2 network under illumination. The values for current and voltage are less than the idealized graphs; however these graphs are only used as a reference point to verify similarities in the curve shape. The slight scatter between specimens—particularly the minimal drop in specimen 2 despite a visible crack after annealing—suggests that the porous film morphology dominates performance, and minor defects do not catastrophically impair current transport.

5.1.2 Power–Voltage Relationship

Multiplying the instantaneous I–V data yields the power–voltage (P–V) curves shown in Figure 2. Each curve peaks at a bias of roughly 0.03–0.05, corresponding to the maximum power point (MPP) where the product $P = I \times V$ is maximized. Normalizing by the electrode area and comparing to the 800 W m^{-2} illumination gives the power densities and efficiencies

listed in Table 2. Specimen 3 achieved the highest power density of 3.68 W m^{-2}, or 0.46% efficiency, likely due to its most uniform dye uptake and optimal film thickness. Specimens 1 and 2 exhibited slightly lower efficiencies (0.40% and 0.38%, respectively), but all three fall within the typical range for anthocyanin-sensitized cells under our lab conditions.

5.2 Sources of Error

Several factors contributed to uncertainty and deviation from ideal performance:

- Film thickness and uniformity: Manual spreading with a pipette edge can introduce local thickness variations. Regions that are too thick may crack during annealing (as in specimen 2), while thin spots reduce light absorption and electron injection.
- Dye adsorption variability: The 10 min immersion in crushed-berry extract can yield nonuniform anthocyanin coverage if residues or pulp particles adhere unevenly. Incomplete rinsing may also leave residues that alter surface chemistry.
- Electrolyte distribution. The dropwise introduction of iodide solution and manual alternating of clips can result in nonuniform filling of the interstice, affecting charge transfer rates at the counter electrode.
- Light intensity fluctuations: Our laboratory lamp can vary in output over time and position; small shifts in slide placement alter the incident flux, impacting both I_{SC} and V_{OC}.
- Measurement uncertainty: The digital multimeter and potentiometer have finite resolution and calibration error ($\pm 0.5\%$ in current, $\pm 0.2\%$ in voltage), which propagates into the calculated power and efficiency values.
- Thermal effects: As noted in the manual, the cell temperature can rise under illumination, causing up to a 40% drop from the peak power over time. We observed a slow decline in current during extended measurements despite keeping the lamp exposure under five minutes per trial.

Overall, while our dye-sensitized solar cells demonstrate the expected qualitative behavior, tighter control of film deposition, dyeing, and measurement protocols would be required to push efficiencies closer to literature values for anthocyanin-based devices.

6 Conclusion

In summary, the anthocyanin-sensitized TiO_2 cells exhibited a maximum average power of 6.0 W at 0.065 V under 800 W/m^2 illumination, corresponding to an average efficiency of 0.413% (mean power density 3.03 W/m^2). The I–V characteristics display the expected non-linear current–voltage relationship governed by internal resistance, while the P–V curves peak near the maximum power point (MPP) between 0.03 and 0.05 V, confirming optimal load conditions. Specimen 3 outperformed the others, achieving a peak power density of 3.68 W/m^2 (0.459%), likely owing to its more uniform film morphology and enhanced dye adsorption. Average photovoltaic parameters were $I_{SC} = 8.97 \pm 0.70$ mA and $V_{OC} = 0.0533 \pm 0.0006$ V, in agreement with the characteristic curves in Appendices 2 and 3 of the lab manual. Systematic uncertainties—film-thickness heterogeneity, electrolyte distribution, lamp-intensity fluctuations, and thermal effects—contributed to data scatter and limited absolute efficiency. Overall, these results validate the idea of low-cost, bio-derived dyes for photovoltaics, however, much more research would be needed to optimize for a truly efficient solar cell.

References

[1] G. P. Smestad and M. Grätzel, *Demonstrating Electron Transfer and Nanotechnology: A Natural Dye–Sensitized Nanocrystalline Energy Converter*, Journal of Chemical Education, vol. 75, no. 6, pp. 752–755, 1998.

[2] The Green Optimistic, *How to Make a Solar Cell*, April 13, 2010. `https://www.greenoptimistic.com/how-to-make-solar-cell-2-20100413` (accessed April 20, 2025).

7 Appendix

7.1 Appendix 1

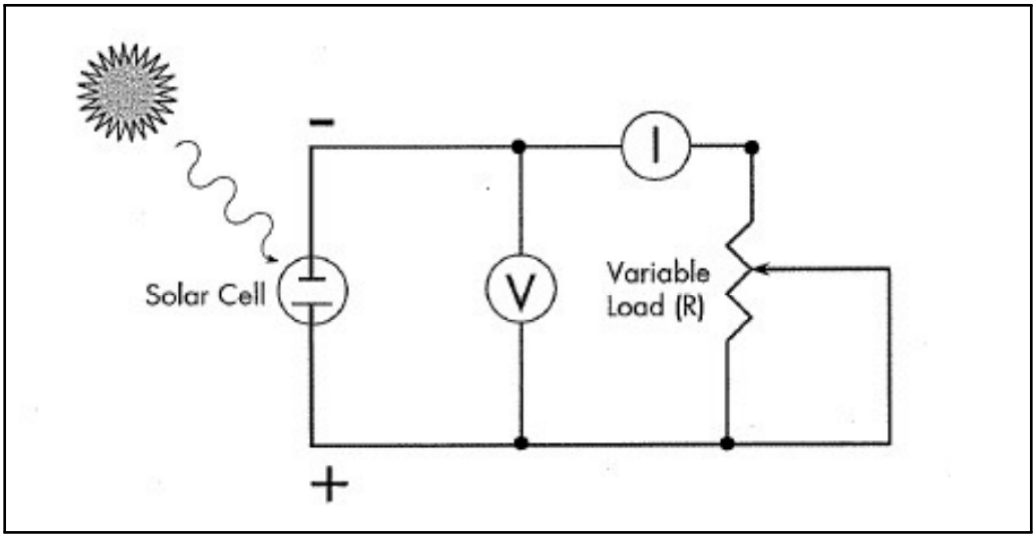

Figure 3: Circuit made for analysis

7.2 Appendix 2

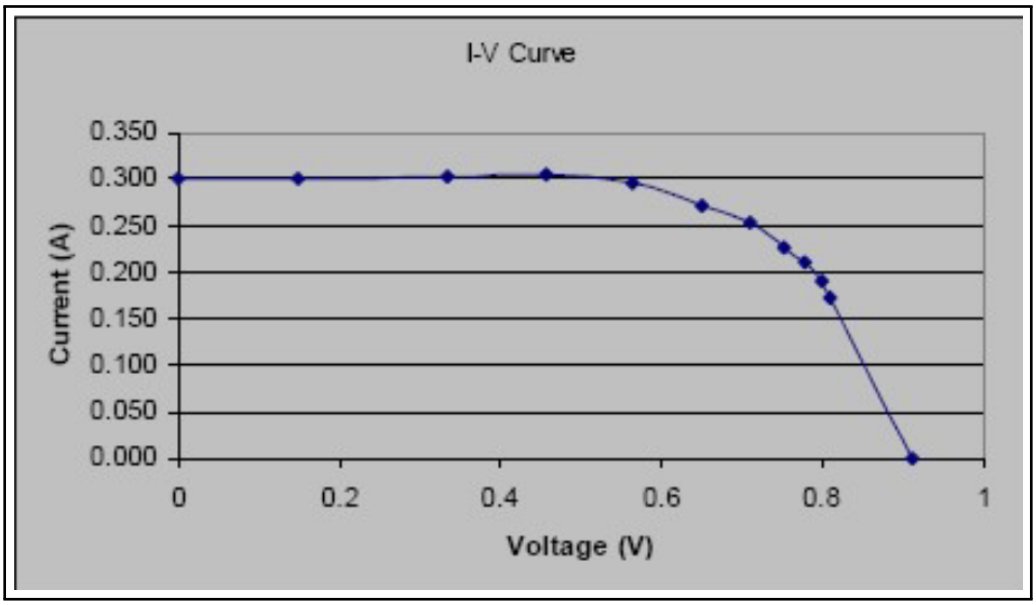

Figure 4: I-V curve from manual

7.3 Appendix 3

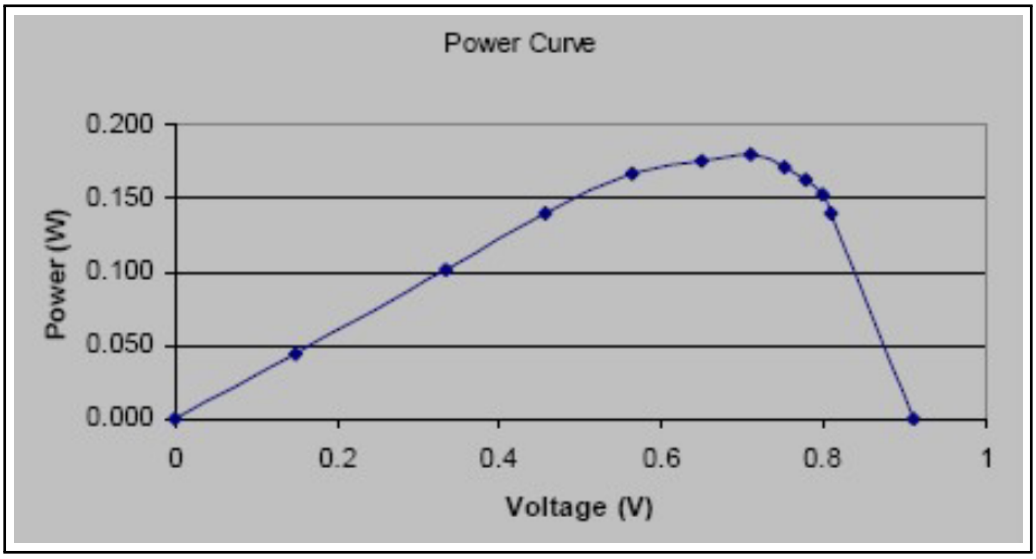

Figure 5: Power curve from manual